AALBORG UNIVERSITY
DENMARK

Angular Distribution of Cellular Signals for UAVs in Urban and Rural Scenarios

Izydorczyk, Tomasz; Tavares, Fernando Menezes Leitão; Berardinelli, Gilberto; Bucur, Madalina Cristina; Mogensen, Preben Elgaard

Angular Distribution of Cellular Signals for UAVs in Urban and Rural Scenarios

Tomasz Izydorczyk[1], Fernando M. L. Tavares[1], Gilberto Berardinelli[1], Mădălina Bucur[1], Preben Mogensen[1,2]

[1]Department of Electronic Systems, Aalborg University (AAU), Denmark

[2]Nokia Bell Labs, Aalborg, Denmark

Email: ti@es.aau.dk

Abstract—Spatial channel characterization of a cellular Unmanned Aerial Vehicle (UAV) Air-to-Ground (AG) communication link is a vital step to understand the potential of beamforming in the take-off zone, when a UAV flies in the vicinity of other objects. In this paper, we evaluate the variation of mean Angle of Arrival (AoA) and Angular Spread (AS) with height based on the experimental measurements using live Long Term Evolution (LTE) networks. The LTE signals are recorded at different heights from a ground level up to 40 m in rural and urban environments. Space-Alternating Generalized Expectation-Maximization (SAGE) algorithm is used for the estimation of the angular parameters. Results show similar mean AoA at different heights, with less than 55 degrees deviation in urban environment and no more than 20 degrees change in rural scenarios. Observed AS is reduced to less than 30 degrees at increasing heights as the Line of Sight (LoS) propagation becomes dominant. However the comparison between urban and rural environments clearly indicates the presence of relevant multipath components in the urban scenarios even 20 m above the rooftops level.

Index Terms—angular spread, UAV, LTE, measurements

I. Introduction

Reliable connectivity is vital to ensure foregoing development of Unmanned Aerial Vehicles (UAVs) as low altitude platforms in safety, security or delivery applications. Nowadays, most of the commercially available UAVs use proprietary communication systems working in the Industrial, Scientific and Medical (ISM) bands for Air-to-Ground (AG) communication. These communication methods are not easily adaptable when UAVs are to be reliably controlled over large distances in beyond visual Line of Sight (LoS) scenarios. Existing cellular networks are an encouraging solution given their world-wide deployment [1]. Their major drawback lies in their design principle to provide ubiquitous connectivity for ground users.

It is important to characterize the radio channel to understand the limitations of cellular connectivity for UAVs. Widely-used terrestrial channel models [2],[3],[4] were created for ground-level communications and as shown for example in [5], are not extendable for flying UAVs. The study in [6] presents a comprehensive survey over research activities on UAV channel characterization. Empirical research focusing on a cellular bands, as presented in this work, is mostly related to large-scale fading statistics for AG channel or its small-scale fading distribution. Deterministic and stochastic radio channel characterization focus also on a LoS probability estimation based on the environment and UAV's flight height.

Authors in [7] report that at sufficient heights, path loss on the AG link approaches the free space model due to a high LoS probability. This leads to increased interference levels as more signals from strongly interfering cells are received [8]. Network [1] and receiver side [9],[10] beamforming were identified as possible solutions to mitigate this interference, as transmit/receive energy can be focused in a desired direction. Their applicability is thus strongly dependent on the common LoS assumption of the AG link at the UAV's flying heights.

Even though, in most applications the UAV is expected to fly at the higher heights, in some scenarios ('last-mile' delivery services, disaster recovery) and during take-off or landing procedures it will be surrounded by infrastructure where LoS propagation assumption can be violated. The potential of using beamforming in these scenarios depends on spatial channel characteristics. In [10], a fixed-beam solution was proposed and evaluated with system-level simulations, in which different number (2, 4 or 6) of fixed beams (with 90° or 50° beamwidth) were used to quantify the UAV performance. Even though the presented results are promising, Angle of Arrival (AoA) and Angular Spread (AS) characteristics at different flying heights need to be better studied, in order to investigate the potential of beamforming solutions. Only by measuring the AS of incoming signals and its AoA stability, the optimal beamwidth can be found and the design questions on, for example, periodicity of beam selection be addressed. To the best of the authors knowledge, there were no experimental studies focused on spatial signal characterization at the so-called *take-off heights* - spanning from the ground level up to the heights where only LoS propagation can be assumed. Understanding the propagation characteristics in the take-off zone is indeed important for addressing the possibility of maintaining a reliable connection in this intermittent flying phase.

In this paper we empirically study the small-scale spatial characteristics of a UAV channel at the take-off heights based on measured live cellular signals. Multi-antenna Universal Software Radio Peripheral (USRP)-based setup and Space-Alternating Generalized Expectation-Maximization (SAGE) algorithm are used for Long Term Evolution (LTE) signal measurements and AoA and AS estimation from the ground-level up to 40 m in different propagation environments. These two aspects are presented as a part of a research project

focused on a complete UAV channel characterization based on large scale measurement campaigns using live LTE networks.

The rest of the paper has the following structure. In Section II the measurement procedure is described. The description of the post-processing, from signal decoding up to the AS computation is presented in Section III. Section IV discusses the obtained small-scale spatial channel characteristics. The work is concluded with Section V.

II. MEASUREMENT METHODOLOGY

A. Hardware setup

The block diagram of the measurement setup, previously described in [9], is shown on Figure 1. A sixteen antennas Uniform Circular Array (UCA), connected with eight dual-port USRP 2953R boards is used to record the cellular signals. The boards are connected with a data hub PXI-8820 controller using a PXIe-1085 chassis.
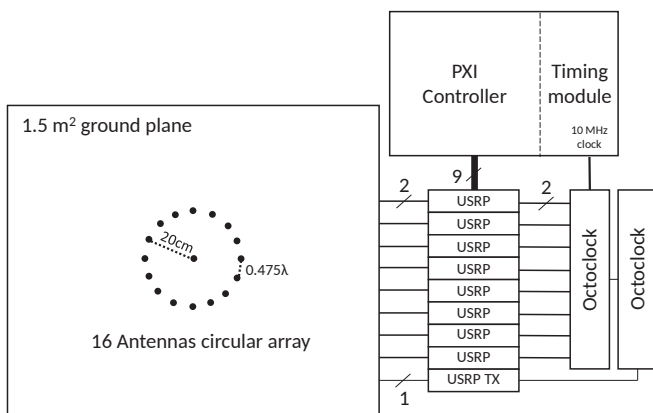

Fig. 1. Measurement setup schematic

Since the main target of this study is to evaluate the spatial channel characteristics, it is inevitable to use a large antenna array to achieve good spatial resolution. The concept of using an actual UAV was quickly ruled out due to the payload limitations, as each of the antennas require its own receive (RX) chain. In addition, advanced channel estimation algorithms including SAGE are usually time consuming and not suitable for the real-time flights using a battery-limited UAV. The main advantage of using our setup is the possibility to record a large amount of data without any real-time processing. One of the unforeseen benefit is the fact that recorded samples can later be used as input in a wide range of activities ranging from channel propagation studies to advanced transceiver design.

1) Antenna array: An UCA composed of sixteen monopole antennas was manufactured to record signals from the Downlink (DL) part of LTE Band 3 used by two Danish mobile operators (center frequencies of 1.815 GHz and 1.87 GHz). The circular radius is 20 cm, which corresponds to a wavelength $\lambda = 0.1625$ m and antenna spacing 0.475λ. The reason for using an UCA rather than a linear array, is its ability to scan the incoming signals in all 360° without ambiguity.

The number of antennas was selected as a trade-off between setup complexity and achievable minimal detection resolution of 22.5°. The UCA is installed on an aluminum ground plane and is connected to the USRP boards using three meter-long RG233 cables.

2) USRPs and PXI controller: Eight USRP 2953R boards record the cellular LTE signals at 40 MS/s and stream the I/Q samples to the PXI controller. Spatial channel estimation studies require perfect time/frequency/phase alignment among all antenna elements. Time and frequency synchronization was achieved by generating the external 10 MHz clock by the timing module NI PXIe-6674T and redistributing it to all boards by two Octoclocks CDA-2990. To achieve a tight phase synchronization between all USRP boards, a method inspired by [11] is introduced. An additional USRP board is used for transmission of a single-tone out-of-band signal from the omni-directional antenna placed at the center of the array. Assuming perfect antenna patterns, all sixteen antennas receive the calibration tone at the same time and with the same phase. By using one of the antennas as a reference, the random phase offset of each USRP board can be compensated. The described procedure was shown to lead to a phase offset error below 3°.

3) Assembled setup: The described setup was assembled in a metal structure and was safely lifted using a crane as can be seen on Figure 2. The ground plane with the installed antenna array was attached to the external of the structure. The antenna array was additionally covered by a hemisphere radome to prevent any short-circuit in case of rain. The radome was tested to be transparent for the radio waves at the measured frequency.

B. Measurement campaign

Measurements were conducted during a two-day campaign in Aalborg, Denmark. Seven different measurement locations, shown in Figure 3, were selected. Two of the measurement locations were in a rural area with limited building density, but still within the coverage area of two Base Stations (BS) located in a close proximity. The remaining five locations were distributed in the urban part of Aalborg in residential and industrial areas. Such choice allows us to sample various propagation environments where a UAV may fly in and compare their spatial channel characteristics. The average transmitter height in Aalborg, of the BS towers operating at the recorded frequency is 26.3 m and the average antenna downtilt is 5.3°. The Inter-Site Distance (ISD) is only 580 m, leading to the measurement equipment being surrounded by BS in all urban locations. A reader is referred to the Section II in [12] for detailed description of the measured environment.

In each location, the designed setup was lifted using the crane from the ground level up to a 40 m height. 100 ms snapshots of two LTE networks in a 1.8 GHz band were taken at every 5 m step starting from the ground. At each height the measurement equipment was stabilized using robes to avoid unintended turning due to the weather conditions, which could affect the AoA estimation. For each of the network operators, an average of eight snapshots were recorded at each

Fig. 2. Assembled setup (top-right) lifted in various environments

height. To avoid signal blockage and self-shadowing due to the location of the antennas and the metal cage, measurements were repeated in two different antenna orientations - upwards and downwards as can be seen on Figure 2. On average 156 snapshots were taken per location.
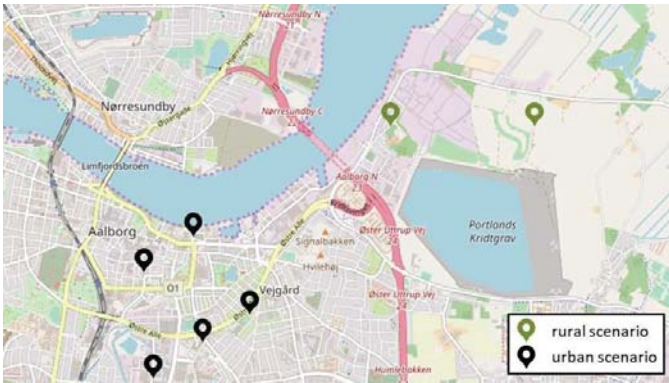

Fig. 3. Map of measured locations in Aalborg, Northern Denmark

III. POST-PROCESSING

In this section the entire post-processing is described starting from the raw acquired data up to angular spread calculation. The method is analogous to the approach presented in [13]. The received and phase calibrated sixteen data streams are used to decode LTE signals in order to obtain Cell-Reference Signals (CRS). Then the original CRS pattern is reconstructed based on received Master Information Block (MIB) and subtracted from the received CRS such that only the received channel information is used by SAGE [14] algorithm to estimate the received signal parameters. Finally, AS can be calculated based on results obtained from multiple snapshots. In the next subsections a description of each step is provided.

LTE receiver: Data recorded independently for each snapshot is provided as an input to a Matlab software that runs the LTE receiver processing. The first step is the initial synchronization to the cell with highest correlation measured over synchronization signals. Next, after time/frequency offset correction, the MIB is decoded using the Maximum Ratio

Combiner (MRC) equalizer. Based on the information encapsulated in a MIB payload, received signal is downsampled to the correct sampling rate and the CRS grid is recovered. To avoid estimation uncertainty, a Signal to Interference and Noise Ratio (SINR) of System Information Block 1 (SIB1) is computed. An empirically-found threshold is imposed and all the snapshots with SINR lower than 0 dB are discarded.

SAGE algorithm: SAGE is an Expectation-Maximization (EM) type of algorithm capable of accurate estimation of complex gain α_i, delay τ_i, azimuth AoA φ_i and doppler ν_i for each estimated propagation path i. Path's gain and respective AoA are of particular interest in this study. For each recorded snapshot, SAGE is initialized to estimate a large number of paths. We set $N_{\mathrm{paths}} = 50$ paths in this study. Received, noisy CRS grid is provided as an input to the SAGE algorithm together with regenerated 'true' transmitted CRS pattern based on information recovered from the MIB. After ten iterations of the algorithm, from the estimated gain-AoA pairs, these with the path gain minimum 15 dB below the strongest path are excluded and treated as noise. Imposed number of iterations and cutoff threshold, come from a sensitivity study based on a preliminary simulation analysis.

When SAGE processing is complete for all the snapshots recorded at the given height, the AS can be estimated. To avoid the signal wrap-up around 0º, estimates for all snapshots are angle-shifted such that the angle of the strongest path is 180º. Figure 4 depicts two example sets of SAGE results that reflect different propagation conditions: LoS (left) and multipath (right). The presented results show the combined SAGE estimates from all the snapshots recorded at the same height (40 m and 30 m respectively) in an urban environment. The presented example of multipath propagation will be further commented later, when obtained results are discussed.
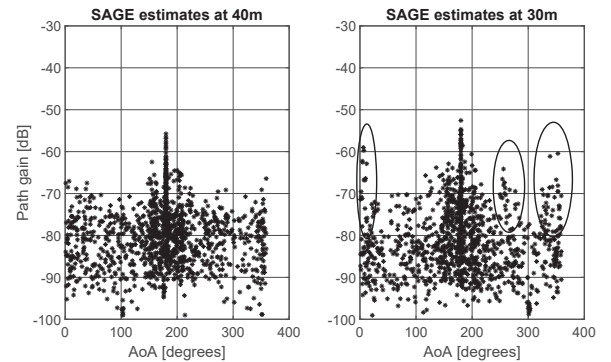

Fig. 4. Typical set of SAGE results with dominant LoS (left), and multipath propagation (right)

Angular Spread estimation: In this work, the method proposed by [15] and used among others in [16], [17] is applied. Angular spread AS is computed as below:

$$AS = \sqrt{\frac{\sum_{k=1}^{N_{\mathrm{snapshots}}} \sum_{i=1}^{N_{\mathrm{paths}}} |\varphi_{k,i} - \bar{\varphi}_k|^2 |\alpha_{k,i}|^2}{\sum_{k=1}^{N_{\mathrm{snapshots}}} \sum_{i=1}^{N_{\mathrm{paths}}} |\alpha_{k,i}|^2}} \qquad (1)$$

where $N_\text{snapshots}$ is a number of snapshots recorded at the given height, $\alpha_{k,i}$ and $\varphi_{k,i}$ are the estimated gain and azimuth AoA for each path i and snapshot k. $\bar{\varphi}_k$ is the mean Angular Power Spectrum (APS) for snapshot k calculated as:

$$\bar{\varphi}_k = \frac{\sum_{i=1}^{N_\text{paths}} \varphi_{k,i} \left| \alpha_{k,i} \right|^2}{\sum_{i=1}^{N_\text{paths}} \left| \alpha_{k,i} \right|^2} \qquad (2)$$

IV. SPATIAL CHANNEL CHARACTERIZATION

A. Estimation of mean Angular Power Spectrum

The mean direction of the APS is one of the key parameters in beamforming operation, as this is the direction towards which the beam should be pointed to capture the most of the incoming signal energy. Its height dependency provides an input on the required beamwidth such that selected direction can remain constant during vertical movement of a UAV provided that mean APS fluctuations are smaller than the selected beamwidth. On the other hand, if the fluctuations are large and the mean direction of the APS encounters major changes with height, a UAV would require to perform frequent beam selection, which may be infeasible in the practical systems and would compromise the reliability of the communication link.

Figure 5 presents the geometrical representation of the mean deviation of APS (Δ_APS), defined as the difference in a mean azimuth direction of the incoming signal recorded at the 40 m and a given height. Mean APS at the 40 m is averaged over all snapshots and used as a reference value since it most likely represents the LoS direction towards the serving cell. Then for all remaining heights, their mean APS and Δ_APS can be computed. This study requires the same signal to be decoded at each height, as signals coming from different BS would have a different mean direction.
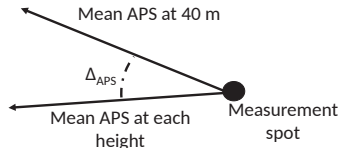

Fig. 5. Geometrical representation of mean APS deviation

Figure 6 presents the variations of the mean APS with respect to the height. There are two locations with a gap in the curves (15 to 20 m and 40 m in Urban 3 and 25 m in Urban 1) meaning that the signal from the target cell was not decoded at these heights due to the high level of interference from surrounding BSs. Apart from the measurements taken in the Urban 2 spot (which coincide to be the most-dense location surrounded by tall buildings), the observed deviation is small at the higher heights and only increase at the lower heights (below 15 m) when surrounded by the infrastructure. In all locations, the mean signal direction did not change more than 60°. In rural areas the observed change was even smaller and did not exceed 22°. In a real development, this would indicate, that unless surrounded by the tall buildings, the target beam direction found at the flying heights can be

kept constant throughout the UAV's descend and the beam scan procedure does not need to be performed very frequently. On the other hand, the strategy of using a fixed beam with large beamwidth (as 60°) can negatively affect the receiver performance as more interfering signals can potentially be received, thus reducing the SINR.
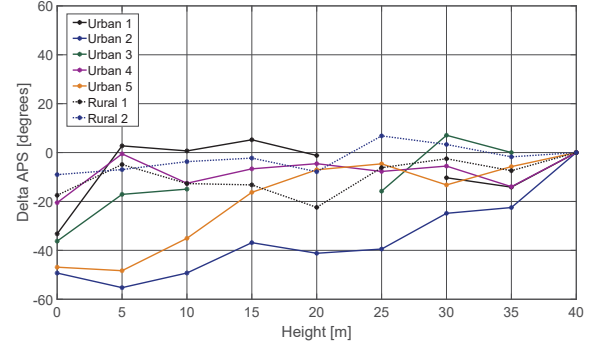

Fig. 6. Measured mean Angular Power Spectrum deviation at different heights

B. Estimation of Angular Spread

AS is the metric which is used to characterize the energy spread of the incoming signal in the spatial domain around its mean direction. It is one of the metrics, which can provide an input on the required beamwidth, sufficient to capture most of the incoming signal power. Its height dependency can be helpful to understand what is the required clearance over the rooftops when LoS propagation becomes dominant, or in other words, down to which height a landing UAV can rely on LoS links and beamforming before entering a rich multipath scenario.
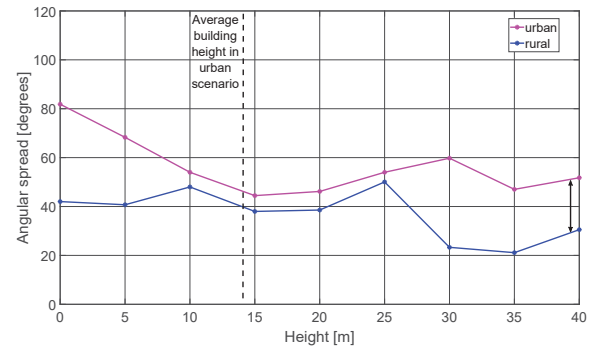

Fig. 7. Measured angular spread at different heights

Figure 7 presents the overall AS, estimated at different heights, for the different environments. In urban scenario, there is a clear descending trend as the UAV flies higher. At the ground level (0 to 10 m) there were multiple snapshots with multipath signal propagation coming from widely separated angles, contributing to the fairly high values of the AS. It is worth to mention, that the overall AS computed for these heights was 69°, which well corresponds to the 68° - the

mean AS value proposed in 3GPP channel model [2]. As the UAV flies higher than the rooftops (15 m and higher) the LoS propagation becomes dominant as AS decreases.

A small increase in AS is observed at 30 m in the urban locations. SAGE estimates obtained from snapshots recorded in this scenario at 30 m are shown at the right side of Figure 4. Three multipath clusters, marked in the figure, can be visually identified based on the quantity of estimates and their path gains. They are most probably caused by reflections from the rooftops. These multipaths contribute to the larger estimated AS. Analysis for larger heights (see one example on the left side of Figure 4) does not reveal the identifiable multipath clusters.

Angular spread measured in the rural scenarios is generally lower than the one estimated from the urban locations, and does not depend on the height. As expected, in the rural area, due to the absence of scatters in the vicinity of the measurement equipment, estimated AS is low even at the lower heights and there is only a slight decrease observed at the highest measurement positions. While comparing the AS estimated at 40 m for both scenarios (as indicated by the arrow on Figure 7), there is more than a ten degrees difference, with the rural AS being narrower. It clearly indicates, that even a 20 m clearance over the rooftops is not sufficient to assume only LoS propagation as obtained results clearly show the presence of some multipath components. In case a so-called pencil beam is used, this can lead to a vast amount of power being left outside of the main beam region.

The low (22.5^o) resolution of our measurement equipment becomes a limiting factor for our study, as in general, the computed AS values for higher heights are larger than expected. However, over 15 m, they are constantly lower than 60°, which can give an indication that this beamwidth is sufficient to capture most of the incoming signal energy.

V. CONCLUSIONS AND FUTURE WORK

In this paper the spatial channel characteristics for cellular UAV air to ground link were analyzed. Mean angular power spectrum was found to not deviate more than 60° between the ground and a 40 m height in scenarios when signals from the same cell were decodable at each height. The deviation was even smaller and did not exceed 22° in rural scenarios. Angular spread was found to be height and location dependent. In urban scenarios angular spread decreases with height as fewer multipath components can be observed, while in rural scenarios the observed decrease is significantly smaller since AS is low also at the lower heights due to limited number of obstructions. The computed angular spread does not exceed 60° at the heights above the rooftops. This further confirms the assumption that communication is dominated by LoS links and in case beamforming is used, gives an indication on the optimal beamwidth. Due to the resolution limitation of our equipment, in the further steps, similar study should be performed with more precise equipment in different measurement environments. The dense-urban 'metropolitan' scenario with skyscrapers should be considered as one of the most challenging environments for UAVs. In addition, the impact of the UAV's fuselage on incoming AS should be investigated.

REFERENCES

[1] Y. Zeng, J. Lyu, and R. Zhang, "Cellular-connected UAV: Potential, challenges and promising technologies," *IEEE Wireless Communications*, pp. 1–8, 2018.

[2] *"Spatial Channel Model for Multiple Input Multiple Output (MIMO) simulations (Rel. 13)"*, January 2016, 3GPP TR 125.996.

[3] *"WINNER II Channel Models"*, Sept 2007, iST-4-027756 WINNER II D1.1.2 V1.2.

[4] *"METIS Channel Models"*, Feb 2015, iCT-317669 METIS, Deliverable D1.4.

[5] K. Daniel, M. Putzke, B. Dusza, and C. Wietfeld, "Three dimensional channel characterization for low altitude aerial vehicles," in *2010 7th International Symposium on Wireless Communication Systems*, Sept 2010, pp. 756–760.

[6] A. A. Khuwaja, Y. Chen, N. Zhao, M. Alouini, and P. Dobbins, "A survey of channel modeling for UAV communications," *IEEE Communications Surveys Tutorials*, 2018.

[7] A. Al-Hourani and K. Gomez, "Modeling cellular-to-UAV path-loss for suburban environments," *IEEE Wireless Communications Letters*, vol. 7, no. 1, pp. 82–85, Feb 2018.

[8] B. V. D. Bergh, A. Chiumento, and S. Pollin, "LTE in the sky: trading off propagation benefits with interference costs for aerial nodes," *IEEE Communications Magazine*, vol. 54, no. 5, pp. 44–50, May 2016.

[9] T. Izydorczyk, M. Bucur, F. M. L. Tavares, G. Berardinelli, and P. Mogensen, "Experimental evaluation of multi-antenna receivers for UAV communication in live LTE networks," *Accepted at Globecom workshops*, Dec 2018.

[10] H. C. Nguyen, R. Amorim, J. Wigard, I. Z. Kovács, T. B. Sørensen, and P. E. Mogensen, "How to ensure reliable connectivity for aerial vehicles over cellular networks," *IEEE Access*, vol. 6, pp. 12 304–12 317, 2018.

[11] M. Willerton, D. Yates, V. Goverdovsky, and C. Papavassiliou, "Experimental characterization of a large aperture array localization technique using an SDR testbench," in *Wireless Innovation Forum Conference on Communications Technologies and Software Defined Radio (SDR11-WInnComm)*, 2011.

[12] R. Amorim, H. Nguyen, J. Wigard, I. Z. Kovács, T. B. Sørensen, and P. Mogensen, "LTE radio measurements above urban rooftops for aerial communications," in *2018 IEEE Wireless Communications and Networking Conference*, April 2018, pp. 1–6.

[13] X. Cai, A. Gonzalez-Plaza, D. Alonso, L. Zhang, C. B. Rodrguez, A. P. Yuste, and X. Yin, "Low altitude UAV propagation channel modelling," in *2017 11th European Conference on Antennas and Propagation (EUCAP)*, March 2017, pp. 1443–1447.

[14] B. H. Fleury, D. Dahlhaus, R. Heddergott, and M. Tschudin, "Wideband angle of arrival estimation using the SAGE algorithm," in *IEEE 4th International Symposium on Spread Spectrum Techniques and Applications Proceedings*, vol. 1, Sep 1996, pp. 79–85.

[15] B. H. Fleury, "First- and second-order characterization of direction dispersion and space selectivity in the radio channel," *IEEE Transactions on Information Theory*, vol. 46, no. 6, pp. 2027–2044, Sept 2000.

[16] Czink, Bonek, X. Yin, and Fleury, "Cluster angular spreads in a MIMO indoor propagation environment," in *2005 IEEE 16th International Symposium on Personal, Indoor and Mobile Radio Communications*, Sept 2005, pp. 664–668.

[17] R. Zhang, X. Lu, J. Zhao, L. Cai, and J. Wang, "Measurement and modeling of angular spreads of three-dimensional urban street radio channels," *IEEE Transactions on Vehicular Technology*, vol. 66, no. 5, pp. 3555–3570, May 2017.